11. GROUP OF LASERS AND PLASMAS

J.T. Mendonça (Head), R. Azambuja, L. Cardoso, M. Cataluna, H. Crespo, J. Davies, J.M. Dias, J. Encarnação, M. Fajardo, G. Figueira, A. Guerreiro, N. Lopes, A.M. Martins, S. Mota, D. Resendes, J.A. Rodrigues, L.O. Silva, G. Sorasio.

11.1. INTRODUCTION

This project included in 2004 activities mainly related with the following research lines:

- Ultra high power, ultra-short lasers[1];
- Theory and simulation on extreme plasma physics[1];
- Studies on complex and space plasmas.

11.2. ULTRA HIGH POWER, ULTRA-SHORT LASERS

11.2.1. Hardware improvements in laser system and target area of the laboratory for intense lasers

11.2.1.1. Diagnostics

A homebuilt SPIDER (spectral phase interferometer for direct electric-field reconstruction) diagnostic (Figure 11.1) was implemented and used to optimize the compressed pulse duration and pulse shape. A thorough study has been undertaken for this purpose, which allowed a better understanding of the role of the several parameters distorting the pulse shape, and how to compensate for them. In what concerns the SPIDER device, an extension of its working parameters into the highly chirped pulse regime was studied.

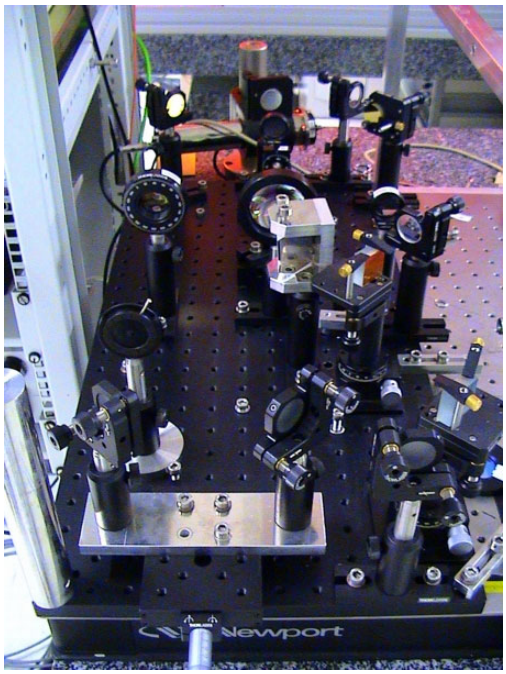

Figure 11.1 – View of SPIDER diagnostic

11.2.1.2. Vacuum pulse compressor

A specially-built vacuum chamber was installed for housing the current grating compressor, compatible with pulse amplification to the 10 Joule level and subsequent compression to the hundreds of fs level, without air-induced pulse distortion. This equipment is composed of a stainless steel vacuum chamber, a mechanically independent internal and external frame where the optical components are attached, a turbomolecular pump and a dry rough vacuum pump (Figure 11.2).

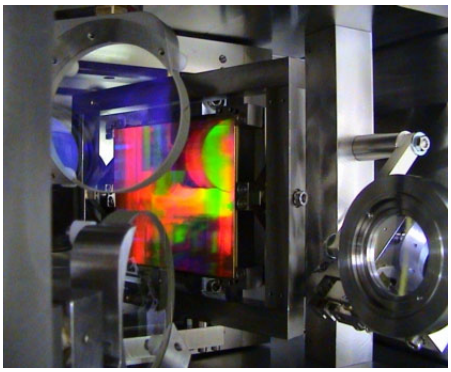

Figure 11.2 – Inside the compressor vacuum chamber, second grating.

11.2.1.3. In-vacuum beam delivery

The new pulse compressor includes a new vacuum beam delivery system (Figure 11.3), composed of a thin polymer window for compressor-target chamber vacuum separation, a gate valve with thick glass window (for low power alignments, a fast gate valve for emergency shutdown and a small vacuum chamber for steering the beam to the target chamber. The compressor vacuum system is automatically controlled by a home made microprocessor based controller. This pulse compressor can be upgraded in future to 50 TW (200 fs) by use of dielectric diffraction gratings.

11.2.1.4. Laser characterization

Following this modification, the laser system was fully characterized (Figure 11.4); in particular given the vertical configuration of the compressor, a new type of tilted pulse front autocorrelator has been successfully tested. A parametrical optimization of the spectral evolution along the laser chain was also performed, in order to minimize the final pulse duration.

[1]In the frame of the project "Keep-in-Touch Activities on Inertial Fusion Energy" of the Contract of Association EURATOM/IST.

Figure 11.3 – View of new in-vacuum beam delivery system

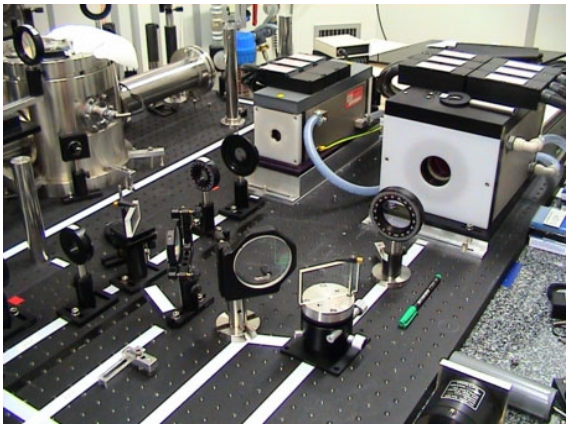

Figure 11.5 – 16 and 45 mm Nd:glass amplifiers

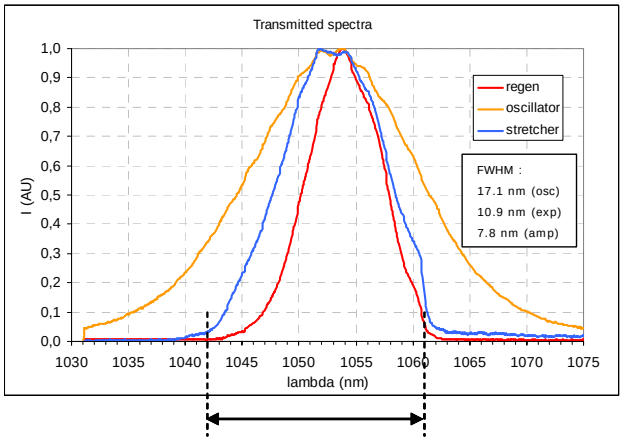

Figure 11.4 – Laser characterization: transmitted spectra at several critical elements in the amplification chain, showing gain-induced spectral narrowing.

11.2.1.5. Nd:glass 45 mm amplifier

This new amplifier was added in April 2004 to the final laser chain, which will allow the envisaged amplification above 10 J (Figure 11.5). Problems in coordinating its triggering sequence with that of the existing Nd:glass amplifier, and a lengthy flashlamp and rod replacement for the latter prevented us from testing both of them together until early 2005, when both situations have been finally solved.

11.2.1.6. Optical parametric chirped pulse amplification (OPCPA)

This work followed its course, and the first experiments are now taking place. A considerable theoretical work was done at this level, concerning the evaluation of ultra broad band optical parametric amplification by using dispersed signal beams. This scheme allows high fidelity amplification of pulses with bandwidths in excess of hundreds of nanometers to the multi-Joule level.

11.2.1.7. Laser modelling

The Miro software package was used for modelling L2I's laser chain; in particular, a thorough study of the best parameters for operating the 16 and 45 mm Nd:glass amplifiers together was undertaken, in terms of pump energy, pulse duration, pulse spectrum and B-integral.

11.2.2. Experiments

11.2.2.1. Electron acceleration

A new experiment on production of plasma channels for electron accelerators has been started. The objective of this experiment was to test the laser triggered-free-plasma-discharge in a differentially pumped gas cell. This is a fundamental step to use this technique in guiding laser pulses at high intensity since it allows reducing ionization-induced refraction of the laser beam at capillary entrance. These first experiments produced no conclusive results on laser guiding due to the difficulty of controlling the pre-pulses with the present laser setup. However, the plasmas lines produced in the gas cell show the same characteristics as those of previous experiments in a filled chamber. The laser system up-grade for 2005 with a new OPCPA arm and better contrast will allow solving the problems found in this experiment.

11.2.2.2. Collaboration with UCLA laser plasma group

A collaboration with the Laser Plasma Group of the University of California – Los Angeles aiming the development of plasma sources for laser plasma interaction was started in 2004. Under this collaboration Portuguese staff has participated in an experiment to test a UCLA-developed plasma source and we started the development of a new generation of plasma sources aiming the production of energetic electron beams by laser-plasma interaction.

11.2.2.3. X-ray lasers and XUV diagnostics

In inertial confinement fusion, high-density plasmas are produced. Optical probes have been widely used to understand laser-produced plasmas, but they have limitations in the study of higher densities such as compressed capsules or high power laser-solid interaction.

These difficulties include high absorption of optical light, strong refraction, and most of all the impossibility of probing beyond the critical density.

X-ray lasers are an ideal tool for studying these types of plasmas, because they can probe higher density regions with novel tools such as XUV interferometer or holography. Highly emitting sources are necessary, however, because one has to overcome the self-emission from the hot dense plasmas. In that context, we have worked in three major fields: improving the emissivity of the XUV source using High Harmonic seeding, designing new XUV diagnostics for plasmas and studying relativistic plasma effects on the propagation of X-ray lasers.

11.3. THEORY AND SIMULATIONS

11.3.1. Theoretical studies of fast ignition inertial confinement fusion

Preliminary theoretical studies of fast ignition using laser generated electron beams were carried out in 2004, leading to the successful submission of a grant proposal on this topic. This project should start in the first half of 2005.

The studies aimed at identifying key physics issues related to the process of fast ignition that need to be understood in order for the scheme to be implemented. Issues that have been considered include energy deposition by a beam with a broad energy spectrum and current limitation by the self-generated magnetic field of the beam.

The original calculations of the electron energy required for the electrons to stop in the core considered a mono-energetic beam, but laser generated electron beams have broad energy spectra. A simple analytical model has been used to estimate the ideal mean energy and the fraction of the beam energy that provides useful heating from the required stopping distance and electron energy distribution.

The minimum current required for fast ignition greatly exceeds the Alfvén limit, so can only propagate while the plasma provides an almost coincident return current. The return current is formed with a separation from the beam current of the order of the collisionless skin depth and the separation then increases as a result of the mutual repulsion of the currents and the decay of the return current due to collisions. The initial current neutralization that can be provided even in the core is insufficient to allow the beam to propagate and the decay time of the return current due to collisions is lower than the pulse duration. Possible solutions to this problem have been considered, and two practical solutions have been identified. A higher mean energy could overcome the problem since this lowers the current and raises the Alfvén limit, which compensates for the expected loss in efficiency. Schemes that could allow an increase in the mean energy without a loss in efficiency are being studied. Multiple beams could overcome the problem since each beam carries a fraction of the total current.

The obvious choice in this case is to use spherical illumination, which theoretically eliminates the problem altogether.

11.3.2. Plasma simulation

The main research theme is high energy density science, or extreme plasma physics. This rapidly emerging field encompasses a wide range of scenarios whose unifying aspects of are established by the methodology followed to tackle the different problems, with a combination of relativistic kinetic theory, plasma physics, accelerator physics, theoretical astrophysics with state-of-the art massively parallel numerical simulations using particle-in-cell codes or hybrid/reduced codes.

The team on extreme plasma physics has developed a strong expertise in plasma simulation codes, theoretical plasma physics, plasma-based accelerators, and advanced simulation techniques. We are now becoming recognized as the leading plasma simulation group in Europe, and achieving worldwide recognition. Collaboration with the leading research programs in the US, and in France in our fields of research is tight and strong, guaranteeing us access to state-of-the-art computing facilities such as the newly commissioned Dawson cluster at UCLA or the IBM SP3 at NERSC, Oakland, California, and the most up to date experimental results.

Our work deals with different aspects of laser-plasma interactions at extreme radiation intensities, ranging from laser-solid interactions to large-scale length plasma accelerators, from fast ignition of fusion targets to shocks in Coulomb explosions of cluster, from theory of stimulated scattering instabilities to sources of energetic protons for cancer therapy.

As a spin-off of the work on inertial fusion energy related problems, we have also extended some of our work to astrophysical problems, namely the nonlinear evolution of magnetic fields generated from collisionless instabilities[2].

The need for a hierarchy of simulation codes capable of covering a wide range of time and length scales has motivated our further development of the hybrid code dhybrid[3].

The CFP cluster has been upgraded to an extra 40 CPU PowerPC G5 over Gigabit Ethernet, for an aggregate cluster size of 80 CPUs, 65 GB RAM (Figure 11.6).

Next sections described the main results obtained in ten research topics.

11.3.2.2. Beam-plasma instability

In fast ignition, huge currents, in excess of hundreds of MA, need to be transported across background plasma whose density varies within more than 4 orders of magnitude. Depending on the properties of the beam, such high fluxes of free energy can drive plasma instabilities. These instabilities can be deleterious if occurring near the coronal region of the plasma, or they can be beneficial if occurring near the core of the compressed fusion pellet.

[2] This work is performed in collaboration with the University of Kansas

[3] This code is being developed in collaboration with the Rutherford Appleton Laboratory.

A systematic analysis of the filamentation instability has been performed by GoLP, using relativistic kinetic theory, exploring the scenarios where this instability can be of relevance. Some of these results have also been applied to the study of equivalent scenarios in astrophysical scenarios, namely gamma ray bursters, with a detailed emphasis on magnetic field generation and nonlinear evolution from collisionless plasma processes.

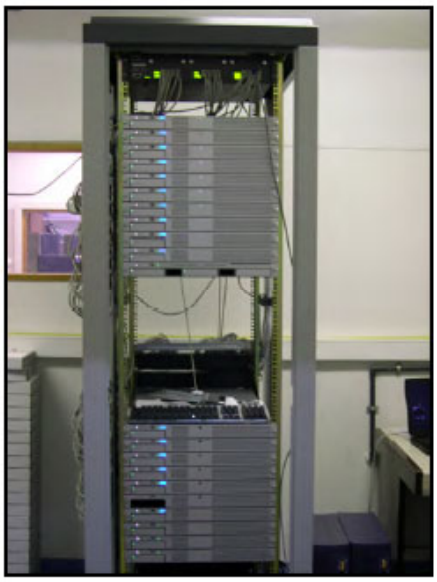

Figure 11.6 – The expp cluster at GoLP.

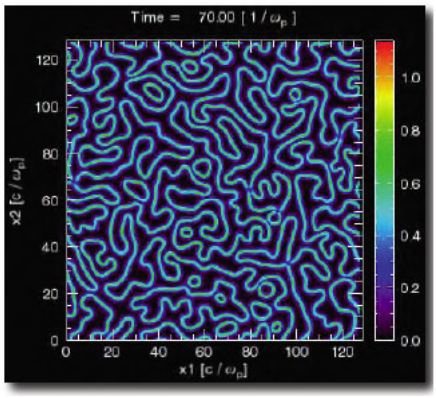

Figure 11.7 – Two-dimensional filamentation instability.

11.3.2.3. Fast electron transport in realistic ICF targets

In 2004, fast electron transport in realistic geometries have been addressed for the first time,. This is a critical issue for fat ignition since all previous simulations have been performed in scenarios not realistic and, thus leading to unphysical results solely associated with boundary conditions. In particular, demonstration that for fast ignition conditions a well-defined electron beam is not formed was made. Furthermore, the role of cone-shaped targets for coupling of the laser radiation to the electrons has been explored.

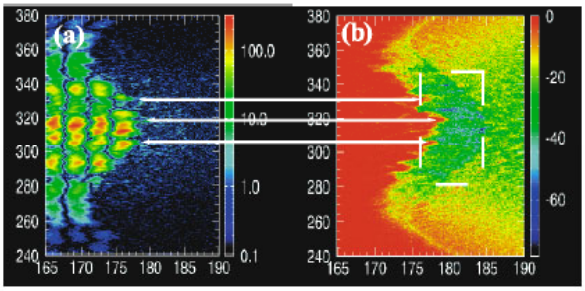

Figure 11.8 – Laser filamention in the interaction region. (a) laser field, and (b) electron density

11.3.2.4. Photon accelerator

In the same way as relativistic plasma waves can accelerate electrons with GeV/cm gradients, they can also upshift photons riding the waves. Such phenomena can be used as a novel way to tune radiation over a wide range of frequencies but also as a diagnostic tool for relativistic structures.

A numerical exploration of the photon accelerator either in a pre-formed plasma or including ionization effects on the short laser pulse driving the wake was performed. As a novel diagnostic the Wigner transform concept was employed, which allows for a clear identification of the relevant physics.

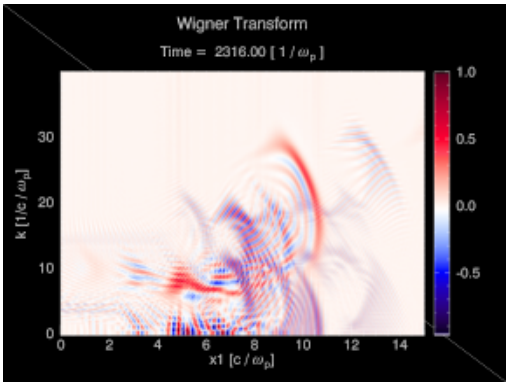

Figure 11.9 – Wigner transform of ultra short laser pulse riding a laser wakefield

11.3.2.5. Osiris 2.0 development

In 2004, IST released osiris 2.0, the novel version of the massively parallel fully relativistic particle-in-cell code osiris, which has been developed within the Osiris consortium. Among the new features, osiris 2.0 includes several ionization models (impact, tunnel, and barrier suppression), binary collisions, and novel laser initialization configurations (Bessel beams, tilted wavefronts). This release of osiris 2.0 has been accompanied by the implementation of a software development infrastructure, based on subversion, for collaborative development, management, and version tracking of the project. In order to achieve performance gains, tight integration between osiris 2.0 and the clusters where this code runs has also been pursued. The

availability of significantly more computational power has also pushed for the development of further features in idl.zamb, the visualization infrastructure for large data sets.

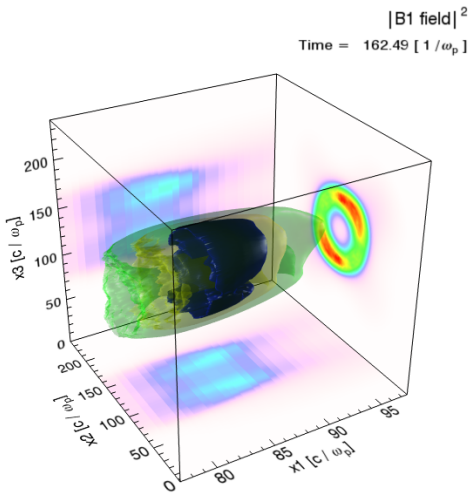

Figure 11.10 – Longitudinal B-field driven by a Bessel beam

11.3.2.6. dHybrid

The first version of dhybrid has now been completed, with major improvements in the hybrid algorithm, and expanded capabilities. The range of scenarios that dhybrid can now deal with has significantly increased from the initial version of dcomet. In this code, the ions are treated as kinetic particles, and the electrons as a massless fluid. The length scale and the time scale is then determined by the ion dynamics thus allowing the simulation of larger/longer scenarios. This code has been employed to study artificial magnetospheres and artificial comets. The current version of dhybrid is now prepared for the next step, which will lead to the parallelization of this code, which will then be the state-of-the-art hybrid code.

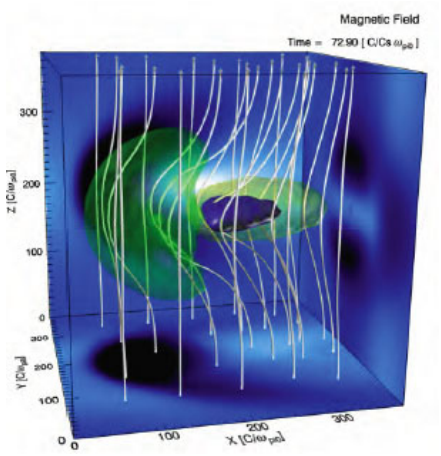

Figure 11.11 – Simulation with dhybrid of an artificial magnetosphere

11.3.2.7. Collisionless shocks for fast ignition and proton acceleration

Demonstration that ultra intense lasers can drive electrostatic shocks that can be very effective in accelerating particles was made. This scenario has been further explored, in order to optimize the proton acceleration mechanisms, and to analyze the possible consequences of these shocks for fast ignition. Significant effort is also been put into the theoretical description of such nonlinear structures, in particular, relativistic collisionless shocks, with shocks velocities comparable to the speed of light.

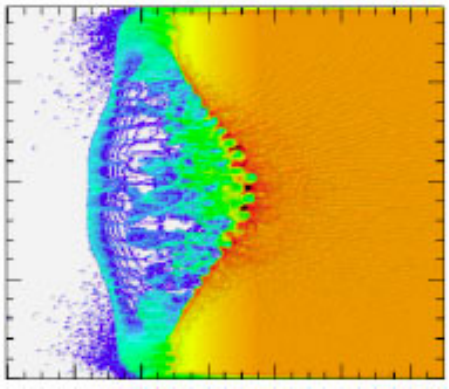

Figure 11.12 – Electron density of collisionless shock from hole boring driven by ultra intense laser in the front surface of solid target (laser is moving from left to right)

11.3.2.8. Explosion of clusters and neutron yield increase from controlled shock shells

A novel technique to control the explosion of nano to sub-micron deuterium clusters was proposed. The possibility to control such explosions opens the way to the increase of the neutron yield due to intra-cluster reactions. This scenario has been explored, optimizing the double pulse technique, generalizing the concept to heteronuclear clusters. The possibility to extend these ideas to other intense radiation sources in the VUV and soft x-ray domains was proposed. Preliminary work on this topic has been pursued.

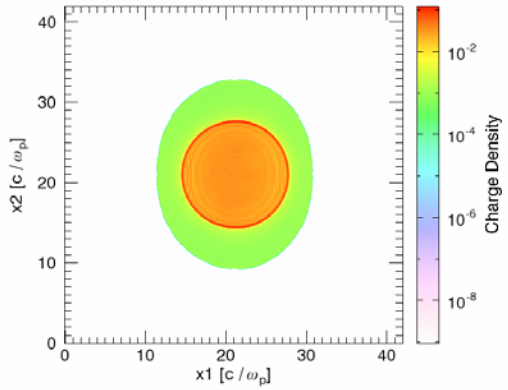

Figure 11.13 – Formation of shock shells: the inner ions overtake the outer ions

11.3.2.9. Blow out, wave breaking and self-injection

The possibility for electron acceleration up to 1 GeV in the laser wakefield configuration in a 1 cm long plasma channel has been identified. The physics that allows for such extreme energies is highly nonlinear and includes the blow-out of the electrons and the formation of an ion channel behind the short laser pulse driving the wake, the wave breaking on the nonlinear plasma wave formed in the trail of the laser pulse, and the self-injection of the electrons into the accelerating bucket.

A detailed theoretical study of these coupled nonlinear phenomena as well as a large number of simulations to test the theoretical model and to interpret the results of experiments under way all over the World have been carried out.

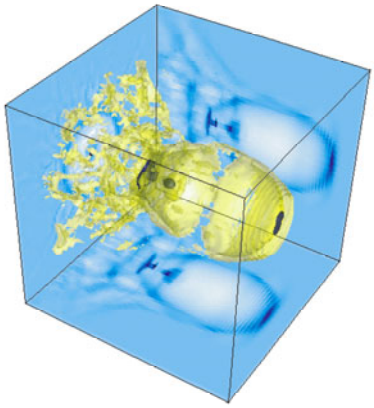

Figure 11.14– Electron density from ultra intense laser blow-out in a preformed plasma

11.3.2.10. B-field generation and the inverse Faraday effect

One of the most interesting phenomena in laser-plasma interactions is the generation of magnetic fields up to the MG level. Different mechanisms can lead to B-field generation in plasmas, but one mechanism is still eluding experimentalists and theorists: the inverse Faraday effect. Detailed numerical simulations of the inverse Faraday effect have been performed, while a new theoretical model including the role of ionization has been studied. Our findings indicate the presence of the inverse Faraday effect, and show that ionization can increase the B-field level.

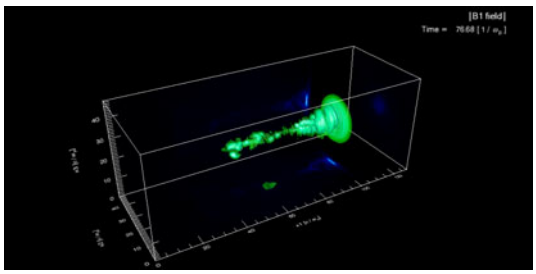

Figure 11.15 – B-field generated by circularly polarized laser in underdense plasma

11.3.2.11. Stimulated scattering instabilities driven by broadband radiation sources

Ultra intense lasers have a large bandwidth either because these pulses are short in duration or due to their interaction with the background media. Furthermore, spectrally broadened long laser pulses (e.g. using random phase plates) are commonly used in ICF since the growth rate for stimulated scattering instabilities is strongly decreased for such laser light conditions. No self-consistent theory exists for stimulated scattering instabilities that accounts for the bandwidth of the radiation source.

A novel theory has been developed by Golp for stimulated scattering instabilities with broadband radiation sources by generalizing the Wigner-Moyal formalism to variable mass Klein-Gordon like systems. In the limit of zero bandwidth (monochromatic pump) the standard results for stimulated Raman scattering for all intensities and all angles have been recovered. The generalized dispersion relation has been derived and explored as a function of the bandwidth of the pump radiation.

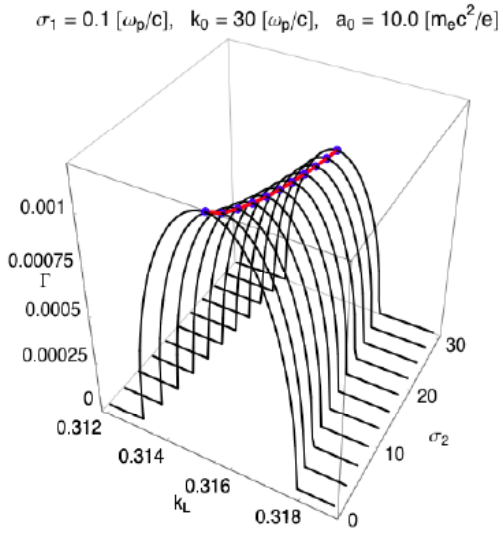

Figure 11.16 – Growth rate for Raman forward scattering including bandwidth effects

11.3.3. Quantum information theory

Together with some work on the foundations of Quantum Mechanics, the research on quantum information theory has been twofold: on multiparticle quantum walks and their algorithmic applications, as well as on how to use electron scattering to entangle magnetic impurities in a solid.

Quantum walks are the quantum version of the random walks. Classically, random walks with *K* particles are equivalent to *K* independent single-particle random walks. In the quantum case though, a walk with *K* particles may contain entanglement, thus offering a resource unavailable in the classical scenario and which can present interesting advantages. Moreover, in the case of identical particles the effects of quantum statistics have to be taken into account,

giving an additional feature to quantum walks that can also be exploited. In this work[4], we show how the entanglement and the relative phase between the states describing the *coin degree of freedom* of each particle will influence the evolution of the quantum walk. In particular, the probability to find at least one particle in a certain position after *N* steps of the walk, as well as the average distance between the two particles, can be larger or smaller than the case of two unentangled particles, depending on the initial conditions we choose. This resource can then be tuned according to our needs, in particular to enhance a given application (algorithmic or other) based on a quantum walk. Experimental implementations were also discussed.

Motivated by the importance of entanglement in quantum computation and in some difficulties to generate it in solid state systems, a scheme to entangle two magnetic impurities (stationary spins 1⁄2) embedded in a solid state system have been proposed[5]. The main idea is to use a ballistic electron as an agent which scatters one the two impurities in succession and entangles them. Being a scattering based scheme, it requires no control over the ability to switch interactions on and off between entities in a solid, as is required by many existing entangling proposals. Moreover, even in comparison to other reduced control proposals, such as those based on scattering or two particle interference, our current scheme has the simplicity that it involves only one mobile entity, namely the ballistic electron, and does away with the difficulty of having to make two electrons coincide at the same place at the same time. This already is focused on how two magnetic impurities embedded in a solid can be entangled by an injected electron scattering between them and by subsequent measurement of the electron's state. The first step was the investigation of an ideal case where only the electronic spin interacts successively through the same unitary operation with the spins of the two impurities. In this case, high (but not maximal) entanglement can be generated with a significant success probability. Afterwards a more realistic description which includes both the forward and back scattering amplitudes was considered. In this scenario, the entanglement between the impurities as a function of the interaction strength of the electron-impurity coupling was obtained. The results led to conclude that our scheme allows us to entangle the impurities maximally with a significant probability (Figure 11.17).

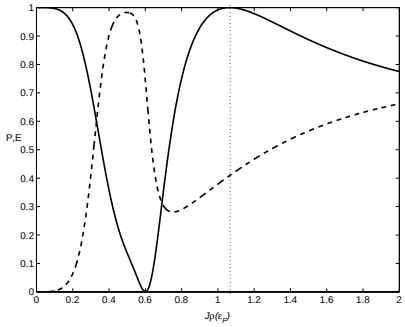

Figure 11.17 – Plots of the probability P (dashed line) of detecting the transmitted electron in the spin down state, and the amount of entanglement E (solid line) obtained between the impurity spins in that case, as a function of the interaction strength $J\rho$ (ε_F), for the realistic scenario of the electron successively scattering of the two impurities.

11.4. STUDIES ON COMPLEX AND SPACE PLASMAS

11.4.1. The science of laboratory colloidal plasmas and mesospheric charged aerosols"[6]

11.4.1.1. Interaction forces and dust dynamics in strongly coupled systems

A large number of laboratory observations reveal the formation of ordered linear chains and sheets composed of charged dust grains levitated in the sheath region of radio-frequency (rf) or dc plasma discharges at very low pressures. At higher pressures, three-dimensional structures are typically formed. Recently, a number of low gas pressure experiments have explored the generation of large amplitude vertical oscillations by lowering either the background pressure or the plasma number density, or by imposing an external force that arises from a low-frequency sinusoidal voltage in the sheath region. A theoretical model has been developed that successfully describes the phenomenology in existing experiments, including the observed self excited oscillations, nonlinear resonance and parametric oscillations. This work was further extended to a self-consistent theory for melting dynamics as well as particle temperature of charged dust grains in plasma sheaths.

11.4.1.2. Waves and instabilities in dusty plasmas

Linear as well as nonlinear mechanisms for the generation of electrostatic and electromagnetic waves in fully and partially ionized dusty plasmas with and without the external magnetic field have been considered. A unified theory describing the effects of charge fluctuations on low frequency phenomena has been developed. The results of this investigation are being applied to the Earth's mesosphere where both negative and positive dust layers are observed. In particular the origin of ELF/ULF waves triggered by positive cloud to ground lightning above mesoscale convective systems has been investigated.

11.4.2. Laser propulsion: ground to orbit launch

The work programme for 2004 involved a review of the state-of-the-art in Laser Propulsion as well as modelling laser thruster flows.

11.4.2.1. State-of-the-art thrusters

The American Lightcraft, the German Bell Thruster, the Japanese Laser driven In-Tube Accelerator (LITA), the Russian Aerospace Laser Propulsion Engine (ASLPE), the

[4] Done in collaboration with S. Bose from UCL and N. Paunkovic and L. Sheridan from the University of Oxford.
[5] Work performed in the frame of the S. Bose from UCL, A. Costa from Universidade Federal de Lavras
[6] In the frame of the European Research Network on Complex Plasmas

Brazilian Laser Supported Directed Energy Air Spike (DEAS), and the American Heat Exchanger Thruster (HX), were reviewed. Of these, only the Lightcraft is a "complete" vehicle. The remaining thruster configurations allow experimental and theoretical study of relevant physical and fluid dynamic issues but are further removed from a thruster application. The Heat Exchanger is technologically close to chemical propulsion and does not take advantage of the high specific impulse which laser propulsion can provide.

11.4.2.2. Laser technology

Full advantage of the promise of laser propulsion for Low Earth Orbit (LEO) requires a high power pulsed laser and consequent efficient propellant absorption, energy confinement, and gas expansion. The real problem is a nonlinear optimization problem involving the propellant, the laser wavelength, the pulse duration, the pulse repetition frequency and the laser power (energy). The selection of the laser wavelength is a critical issue for laser propulsion. Most work to date has concentrated on the 10.6 μm wavelength because of the availability of high power CO_2 lasers. The optimal wavelength will depend on tradeoffs between a variety of parameters, including transmission, absorption, laser efficiency, and the specific mission. Absorption favours longer wavelengths, whereas transmission through the atmosphere and optics favours shorter wavelengths. State-of-the-Art CO2 lasers typically reach 100 kW average power on the order of a few minutes of operation. Closed cycle designs exist which would allow for continous operation.

11.4.2.3. Laser heated flow modelling

Steady laser heated LSD wave flows using LiH as propellant have been modelled. Both an equilibrium and a two-temperature kinetic model were investigated. The resulting structure of the LSD waves have been derived. For completeness, an LSC steady model with H as propellant was also investigated. Thruster performance calculations for the equilibrium LiH model have been obtained. It is seen that the calculated performance is comparable, within factors of 2-3, to the Lightcraft vehicle performance which uses air as propellant. Figures 11.18 and 11.19 present results from the kinetic flow modelling.

11.4.2.4. Trajectory modelling

Numerical simulations were performed to gain insight into the mechanics of laser propulsion ascent trajectories and how these are influenced by the most relevant mission parameters. The simulations were performed using Colvet. This is a WindowsTM application coded in Fortran 95. The vehicle is approximated by a point-mass. There are no moments and the only forces acting on the vehicle are gravity, aerodynamic drag and propulsive thrust. Several interesting results were found in the simulations performed. A simple steering program made of steps and slopes performs close to that of optimized pitch programs. This allows for a small number of parameters to completely define a steering program, greatly decreasing the complexity of analyzing laser propulsion. The general trend of 1kg of payload for every mega-Watt of laser power was confirmed. There is an optimum laser power for a given launch mass, within a given mission. Drag losses strongly influence low mass vehicles. Aerodynamic design should be a major design driver. It is beneficial to use as high specific impulse as possible, as long as it allows enough thrust for a given power setting to lift the vehicle fully loaded. Comparison with flight results shows very good agreement.

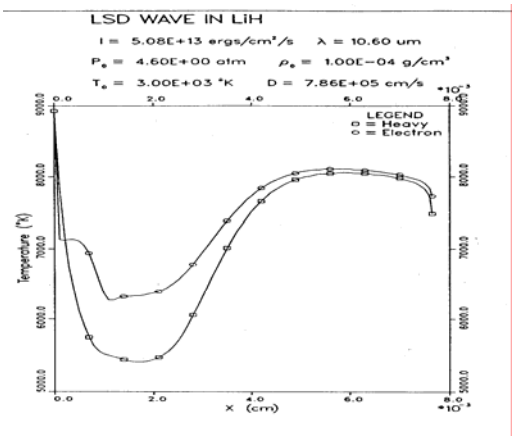

Figure 11.18 - Finite kinetic 2-T temperature profile.

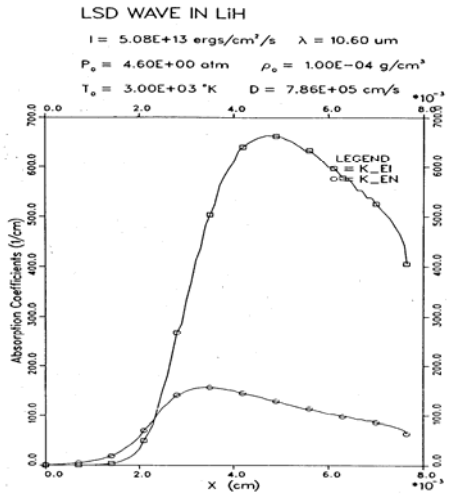

Figure 11.19 - Laser Supported Detonation (LSD) wave absorption coefficients.

11.4.3 Lidar guidance navigation and control (GNC)

The activity involved applied research into the applicability of single photon counting Lidar as an altimeter for both landing and rendezvous missions of a space vehicle. Functional Lidar requirements were determined from mission requirements. Simulation of a complete laser altimeter system was performed including the appropriate transmitter and detector array receiver. The basic equations were applied to this novel altimeter and appropriate design parameters were derived. The figures below (11.20 to 11.22) present typical results, showing the variation of the average laser power and receiver aperture

as a function of laser PRF between 1-30 000 Hz. An array detector with 64 elements is simulated. The range is fixed at 5000 m for a scan angle of 20º. The power decreases monotonically but eventually saturates. At a PRF of 30000 Hz, the transmitter power is 1 Watt, a very acceptable value. The radius increases monotonically but eventually begins to saturate. Even at 30 000 Hz, the upper PRF frequency for single pulse TOF, the detector radius is 3 cm. Current available commercial technology which could implement the design was indicated.

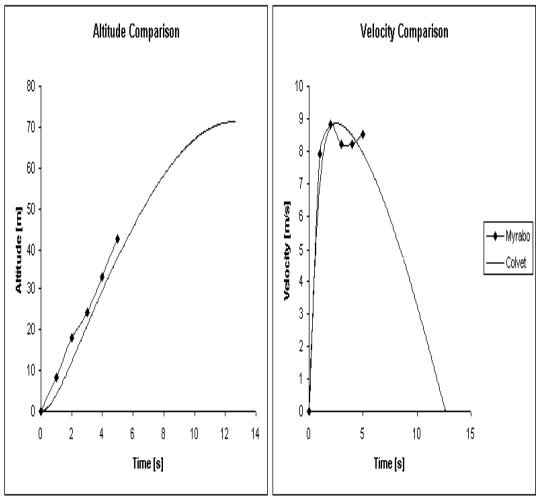

Figure 11.20 - Altitude and Velocity Profile Comparison with Myrabo Flight Results

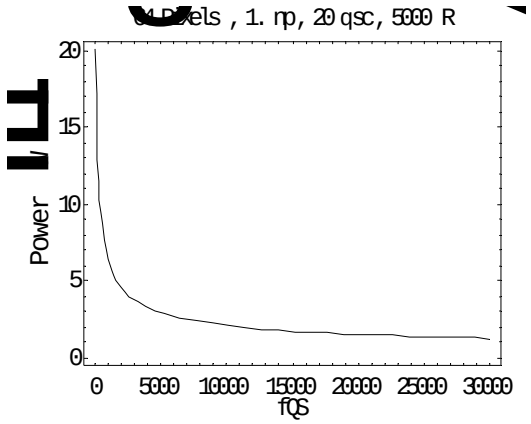

Figure 11.21 - Average Laser Power vs Laser PRF (64 Element Detector) Landing.

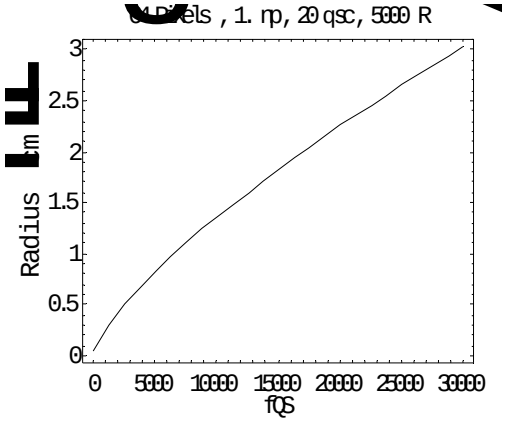

Figure 11.22 - Receiver Aperture vs Laser PRF (64 Element Detector) Landing.